E-Article

Allee Effects and the Evolution of Polymorphism in Cyclic Parthenogens

Magda Castel,[1,2,*] Ludovic Mailleret,[3,4,5,6] Didier Andrivon,[7] Virginie Ravigné,[8] and Frédéric M. Hamelin[1,2]

1. Agrocampus Ouest, UMR 1349 IGEPP, F-35042 Rennes, France; 2. Université Européenne de Bretagne, France; 3. Institut National de la Recherche Agronomique (INRA), UMR 1355 Institut Sophia Agrobiotech (ISA), F-06903 Sophia Antipolis, France; 4. CNRS, Unité Mixte de Recherche (UMR) 7254 ISA, F-06903 Sophia Antipolis, France; 5. Université de Nice Sophia Antipolis, UMR ISA, F-06903 Sophia Antipolis, France; 6. Inria, Biocore, F-06902 Sophia Antipolis, France; 7. INRA, UMR 1349 Institut de Génétique, Environnement et Protection des Plantes (IGEPP), F-35653 Le Rheu, France; 8. Centre de coopération internationale en recherche agronomique pour le développement, UMR Biologie et génétique des interactions plantes parasites, F-34398 Montpellier, France

Submitted November 29, 2012; Accepted August 23, 2013; Electronically published February 10, 2014

Online enhancement: MATLAB code.

abstract: Cyclic parthenogens alternate asexual reproduction with periodic episodes of sexual reproduction. Sexually produced free-living forms are often their only way to survive unfavorable periods. When sexual reproduction requires the mating of two self-incompatible individuals, mating limitation may generate an Allee effect, which makes small populations particularly vulnerable to extinction; parthenogenetic reproduction can attenuate this effect. However, asexual reproduction likely trades off with sexual reproduction. To explore the evolutionary implications of such a trade-off, we included recurrent mating events associated with seasonal interruptions in a simple population dynamics model. Following an adaptive dynamics approach, we showed that positive density dependence associated with Allee effects in cyclic parthenogens promotes evolutionary divergence in the level of investment in asexual reproduction. Although polymorphism may be transient, morphs mostly investing into sexual reproduction may eventually exclude those predominantly reproducing in an asexual manner. Asexual morphs can be seen as making cooperative investments into the common pool of mates, while sexual morphs defect, survive better, and may eventually fix in the population. Our findings provide a novel hypothesis for the frequent coexistence of sexual and asexual lineages, notably in plant parasitic fungi.

Keywords: coexistence, seasonality, dual reproductive modes, strong Allee effect, evolutionary extinction.

Introduction

Sexual reproduction is often associated with ecological functions, such as the formation of structures able to persist, disperse, or both (Williams 1975; Abrahamson 1980). Even in species capable of both sexual and asexual reproduction, that is, cyclic parthenogens, sexual reproduction is often the only way to produce structures able to resist winter frost or summer drought. In aphids for instance, eggs are the only cold-resistant stages (Simon et al. 2002). In the cladocerans *Daphnia* (Tessier and Cáceres 2004) or *Bythotrephes* (Wittmann et al. 2011), diapausing eggs are encapsulated in a cold- and drought-protective envelope. The same applies to cyclically parthenogenetic rotifers (Carmona et al. 2009). Winter survival is also associated with resistance stages in therophyte plants which complete their life cycle during the favorable season and produce seeds to cope with the adverse season. Many plant pathogens, such as fungi and oomycetes, produce thick-walled structures able to cope with adverse environments and to germinate under favorable conditions, for example, oospores in oomycetes and ascospores in fungi.

Beyond the well-known cost of meiosis (Williams 1975), sexual reproduction can have demographic consequences. As an example, the lower the population density, the lower the likelihood of finding a mate. Sexual reproduction therefore entails a positive correlation between one component of growth rate (mating success) and population density, called a component Allee effect (Allee et al. 1949). In fact, mating limitation has been reported as the most common mechanism leading to Allee effects (Gascoigne et al. 2009). These effects associated with sexual stages have been detected in several taxa such as the wild radish *Raphanus sativus L.* (Elam et al. 2007), the estuarine grass *Spartina alternifora* (Davis et al. 2004) and the European gypsy moth *Lymantria dispar* (Vercken et al. 2011). Under some circumstances, such component Allee effects may give rise to extinction threshold population densities, a phenomenon called a strong Allee effect. The occurrence of such

* Corresponding author; e-mail: magda.castel@laposte.net.

Am. Nat. 2014. Vol. 183, pp. E75–E88.
0003-0147/2014/18303-54301$15.00.
DOI: 10.1086/674828

an Allee effect depends on the features of reproductive systems (e.g., overwintering sexual stages, selfing) as well as on social or spatial clustering. Determining whether or not component Allee effects translate into extinction thresholds has triggered numerous studies (Kramer et al. 2009) Yet the consequences of mating limitation have seldom been considered in parasites (Garrett and Bowden 2002; Krkošek et al. 2012).

Organisms having a dual sexual-asexual reproductive mode are expected to be less vulnerable to Allee effects than exclusively sexual ones. Such a mode of reproduction is typical of many parasites, including aphids, oomycetes, and fungi. Interestingly, it has been reported that the level of investment in asexual reproduction is variable within species with obligate sexual reproduction (Simon et al. 2002; Tessier and Cáceres 2004; Carmona et al. 2009). For instance, European populations of the ascomycete *Leptosphaeria maculans*, which causes stem canker (blackleg) on *Brassica* species, are almost exclusively sexual, while western Canadian populations invest more in asexual reproduction (Dilmaghani et al. 2012). In Saskatchewan province, polymorphism in sexual mode of reproduction has even been reported. Polymorphism also occurs in poplar rust, caused by the basidiomycete *Melampsora larici-populina*; in France, several genetic groups with markedly different asexual reproduction levels have been reported (Xhaard et al. 2011). In this study, we focus on polymorphism at such a relatively small spatial scale.

Since asexual and sexual reproduction rely on the production of different structures, one may expect a resource allocation dilemma between them (Chamberlain et al. 1997; Schoustra et al. 2010). High investment in asexual reproduction should to some extent lead to a detrimental effect on sexual offspring quantity (Michelmore and Ingram 1980; Chamberlain et al. 1995) or viability, as repeatedly detected in perennial plants (Vallejo-Marín et al. 2010). A trade-off between asexual reproduction and offspring survival when the host is absent has been reported in natura for several plant pathogenic fungi (Carson 1998; Abang et al. 2006; Sommerhalder et al. 2010, 2011).

Trade-offs between parasite asexual reproduction capacities and survival out of the host have also been previously considered in studies on parasites that produce free-living forms (Gandon 1998; Day 2002; Caraco and Wang 2008), and has for instance been observed in phages of *E. coli* (De Paepe and Taddei 2006). Such a trade-off was theoretically shown to support the emergence of polymorphism in strategies of survival outside the host where parasites relying on direct host-to-host transmission coexist with parasites able to survive through free-living forms (Boldin and Kisdi 2012). A model of evolution of plant pathogens living in seasonal environments showed conditions for coexistence between parasites with very contrasted abilities to overwinter (Hamelin et al. 2011). It also demonstrated that the emergence and maintenance of polymorphism was attributable to negative density dependence at the onset of the epidemic, that is, during primary infections, since it cannot be explained by the trade-off alone (van den Berg et al. 2011).

In cyclic parthenogens, negative density dependence during the season (population regulation through competition for resources) alternates with positive density dependence at the end of the season, that is, component Allee effects associated with sexual reproduction. In other words, population density can be viewed as a common good for mating. Because asexual reproduction trades off with survival, reproducing asexually within the season may be interpreted as a heavy investment in the common good, and investing much in sexual reproduction as a defection. Since cooperation can generate evolutionary diversification (Doebeli and Dieckmann 2000; Day and Young 2004; Doebeli et al. 2004; Doebeli 2011), we wondered whether obligate sexual survival could generate disruptive selection for investment in asexual reproduction, with evolutionary coexistence of sexual (defectors) and asexual (cooperators) lineages.

To investigate this, we model the seasonal dynamics of a pathogen population, using a semidiscrete formalism (Mailleret and Lemesle 2009). The key feature of the model is that within-season asexual reproduction is followed by an obligate sexual episode at the end of season. Sexual survival forms therefore constitute the primary inoculum for the next season. We focus on plant parasitic fungi to make explicit model assumptions but keep the model as simple as possible for the sake of generality. First, we analyze population dynamics over ecological timescales, showing that the component Allee effect associated with sexual reproduction translates into an extinction threshold density for the parasite population, that is, a strong demographic Allee effect. Then, we consider the fate of a mutant differing in its investment in sexual reproduction and describe the complex evolutionary outcomes associated with Allee effects. Finally, we discuss the relevance of these results with respect to observed variability in asexual investment.

Ecology

Model

Let (P, S, I) denote the densities of primary inoculum (sexual survival forms) and susceptible and infected host, respectively. Term T denotes the length of one cycle, $\tau < T$ the time during which the host is present, that is, the growing season length, and n a cycle index. Term N denotes the total host density, assumed constant during a growing season. Finally, sexual reproduction is assumed to result from the interaction between individuals with

compatible mating types. We also consider only two mating types (designated as "−" or "+") as in most species (Billiard et al. 2011). Terms I_- and I_+ denote the densities of hosts infected by − or + mating types, respectively ($I = I_- + I_+$). The following steps of model definition are schematically represented in figure 1.

During Host Presence. Secondary infection dynamics are described as an "SI model" (Anderson and May 1991). New infections occur at a rate proportional to both susceptible host density (S) and infected host density (I). The secondary infection rate β is identical for both mating types. Let $\dot{I} = \mathrm{d}I/\mathrm{d}t$. For all t between nT and $nT + \tau$, the model reads

$$\begin{cases} \dot{I}_- = \beta(N - I_- - I_+)I_-, \\ \dot{I}_+ = \beta(N - I_- - I_+)I_+, \end{cases} \tag{1}$$

where $(N - I_- - I_+) = S$. To keep the model as simple as possible, we have considered that infected hosts remain infectious throughout the season. This simplification fits many plant diseases, such as soilborne fungal diseases (Bailey and Gilligan 1999) or viral diseases (Fabre et al. 2012). The resulting dynamics are mathematically equivalent to logistic growth so that the model is not restricted to plant diseases at this stage.

Transition from Host Presence to Host Absence. At time $t = nT + \tau$, right before hosts disappear, each infected host produces survival forms following sexual reproduction. In fungal plant pathogens, sexual reproduction may result from contact between two adjacent lesions with compatible mating types, or from fecundation by airborne gametes as in, for example, *Melampsora larici-populina*. To keep mathematical tractability, the mating function considered is simply bilinear in the densities of + or − mating types:

$$P(nT + \tau) = \Gamma I_-(nT + \tau)I_+(nT + \tau). \tag{2}$$

During Host Absence. Survival forms P are subjected to a constant between-season mortality rate μ. Then, for all t between $(nT + \tau)$ and $(n + 1)T$,

$$\dot{P} = -\mu P. \tag{3}$$

One can solve equations (2) and (3), leading to

$$P[(n + 1)T] = \Gamma I_-(nT + \tau)I_+(nT + \tau)\mathrm{e}^{-\mu(T-\tau)}. \tag{4}$$

Transition from Host Absence to Host Presence. At the beginning of each new season (time $t = [n + 1]T$), a density N of susceptible hosts is made available to the parasite, for example germinates or is planted. The primary inoculum germinates and infects susceptible hosts, generating

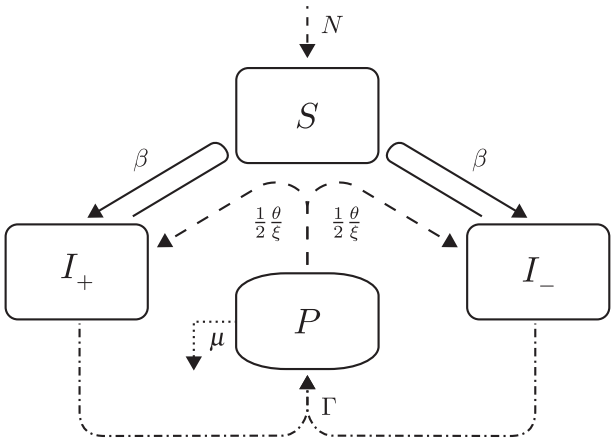

Figure 1: Schematic representation of the different epidemic processes in the seasonal plant epidemic model. Term P (the primary inoculum) denotes survival forms resulting from sexual reproduction of two individuals having compatible mating types. The S and I denote susceptible and infected individual densities, respectively. Dashed lines represent processes occurring at the beginning of the season (plant renewal and primary infections), solid lines represent secondary infections occurring during a growing season, dash-dotted lines represent sexual reproduction occurring at the end of the host growing season, and the dotted line represents mortality of the sexual forms between growing seasons.

− or + progeny in equal probability. The primary inoculum converts into infected hosts with a factor θ/ξ. This conversion factor derives from a model reduction technique (app. A.1) based on the assumption that primary infections occur over a shorter timescale than subsequent plant-to-plant secondary infections (Mailleret et al. 2012). Assuming that θ/ξ is small, the model reads

$$\begin{cases} I_-[(n + 1)T] = \dfrac{1}{2}\dfrac{\theta}{\xi}P[(n + 1)T], \\ I_+[(n + 1)T] = \dfrac{1}{2}\dfrac{\theta}{\xi}P[(n + 1)T]. \end{cases} \tag{5}$$

For the sake of simplicity, we stick to this assumption in the remainder of this section. Appendix A.1 presents the model that was actually used in this study; it is slightly more technical but holds for any θ/ξ value. Thence, the infection cycle (eqq. [1]–[4]–[5]) starts again.

Model Simplification. Equation (5) shows that after the first episode of sexual reproduction, the mating-type ratio remains unbiased forever. In addition, model ([1]–[4]–[5]) can be simplified by setting $I = I_- + I_+$. Let $\chi = (\theta/\xi)(\Gamma/4)\mathrm{e}^{-\mu(T-\tau)}$. The model now reads, for all t between nT and $nT + \tau$,

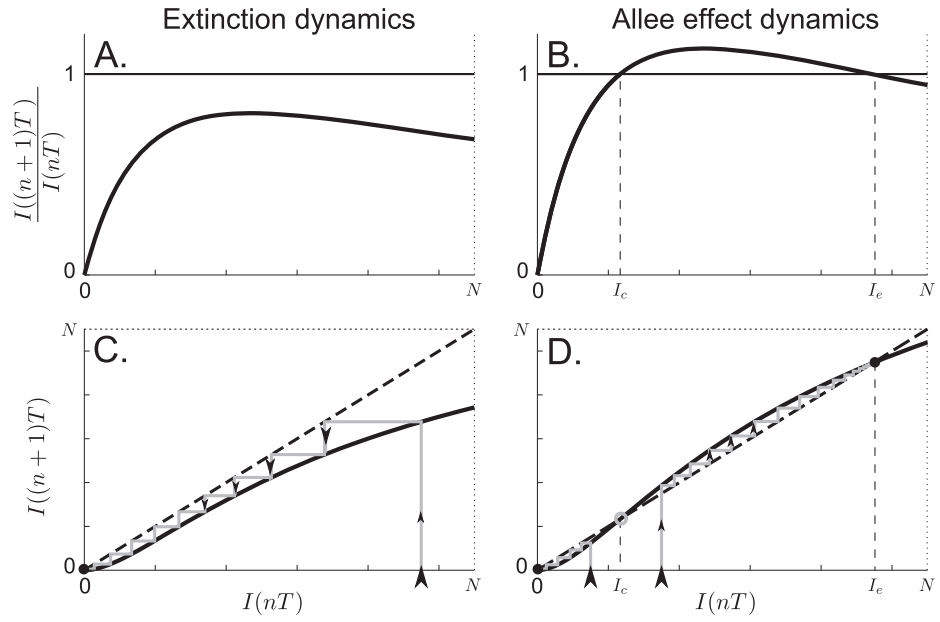

Figure 2: Graphical illustration of the year-to-year model (8) in the two generic cases: global extinction (*left panels*) and bistability typical of a strong Allee effect (*right panels*). *Top row*, year n to year $(n + 1)$ reproductive ratio as a function of infected host density at the beginning of year n. *Bottom row*: cobweb diagrams plotting infected host density at the beginning of year $(n + 1)$ as a function of that at the beginning of year n. Gray squared lines are typical season-to-season dynamics produced by model (8) across years, eventually converging to the disease-free equilibrium (*C* and *D*) or to the endemic equilibrium I_e (*D*).

$$\dot{I} = \beta(N - I)I, \tag{6}$$

and

$$I[(n + 1)T] = \chi I(nT + \tau)^2. \tag{7}$$

Model ([6]–[7]) can be further reduced to

$$I[(n + 1)T] = \chi\left[\frac{I(nT)N}{Ne^{-\beta N\tau} + I(nT)(1 - e^{-\beta N\tau})}\right]^2. \tag{8}$$

The above discrete-time equation maps the density at the beginning of one season $I(nT)$ onto the density at the beginning of the next season $I[(n + 1)T]$.

Strong Allee Effect

At low infected host density ($I \ll N$), equation (8) simplifies to

$$\frac{I[(n + 1)T]}{I(nT)} \approx \chi e^{2\beta N\tau} I(nT), \tag{9}$$

which shows that parasite reproductive ratio increases with infected host density; that is, the parasite population undergoes a component Allee effect. This is a direct consequence of the mating function used in equation (2).

The reproductive ratio $I[(n + 1)T]/I(nT)$, computed from equation (8) as a function of population density $I(nT)$, determines the fate of the parasite population (fig. 2; app. A.2). It may never reach 1 (fig. 2*A*–2*C*), so that the dynamics converge to the disease-free equilibrium ($I = 0$) and the parasite becomes extinct whatever its initial density. If parameter values are such that the reproductive ratio reaches 1 for certain densities (fig. 2*B*–2*D*), equation (8) has three fixed points: the disease-free equilibrium and an endemic equilibrium I_e, which are both stable, as well as a critical unstable fixed point I_c ($0 < I_c < I_e$), separating the dynamics between extinction ($I < I_c$) and convergence to the endemic equilibrium I_e ($I > I_c$). If the reproductive capacities of the parasite are high enough, and provided its initial population density is large enough, it may persist on a year-to-year equilibrium, generating T-periodic epidemic outbreaks. The model cannot show year-to-year cycles or chaotic behavior when a single morph is considered.

Evolution

We will now turn to investigating the evolutionary implications of these Allee effects. Following an adaptive dynamics approach (Metz et al. 1992; Dieckmann and Law 1996; Diekmann 2004), we have derived an invasion criterion for an initially rare mutant phenotype, challenging a distinct resident phenotype.

The secondary infection rate β represents investment in

asexual reproduction, as it is proportional to the number of asexual spores produced per infected individual per unit time within the season. We assumed that β trades off with survival ability. The per capita mortality rate μ is therefore an increasing function f of β. In what follows, we refer to the pair (β, μ) as a single ecological trait which is further assumed to depend on a single multiallelic locus. Mating is also assumed to be coded by a single independent locus. We have focused on a haploid species in which survival forms result from meiosis (Heitman et al. 2007; Coluccio et al. 2008). As a consequence, sexual survival forms inherit each allele from either parental cell with equal probability for both the mating type and the ecological trait.

Evolutionary Invasion Analysis

We have assumed that evolution proceeds through successive mutations arising within a resident population which have reached permanent ecological dynamics, as opposed to transient ones. The dynamics of each emerging mutant can be predicted by deriving an invasion criterion. To this end, we have extended model ([6]–[7]) to two subpopulations (resident and mutant), denoted by subscripts 1 and 2.

Each subpopulation contains both mating-types $-$ and $+$ in equal proportions ("Model"). For instance, $I_1 = I_{1,+} + I_{1,-}$ represents the subpopulation having the ecological trait (β_1, μ_1).

During the season (t between nT and $nT + \tau$), the continuous part is described by

$$\begin{cases} \dot{I}_1 = \beta_1 I_1 (N - I_1 - I_2), \\ \dot{I}_2 = \beta_2 I_2 (N - I_1 - I_2). \end{cases} \tag{10}$$

At the end of the season, offspring is generated from the mating of two parents that have either the same ecological trait, as in equation (7), or two different traits, that is, $I_{1,-} \times I_{2,+} + I_{1,+} \times I_{2,-} = 2 \times (I_1/2)(I_2/2)$. In the latter case, because the parasite is haploid, each offspring has probability 1/2 of inheriting either parental allele for each trait. Therefore, offspring production for each trait, at time $t = nT + \tau$, is

$$\begin{aligned} P_1(t) &= \Gamma\left(\underbrace{\left(\frac{I_1(t)}{2}\right)^2}_{\text{resident} \times \text{resident}} + \frac{1}{2} \times \underbrace{2 \times \frac{I_1(t)}{2}\frac{I_2(t)}{2}}_{\text{resident} \times \text{mutant}} \right), \\ P_2(t) &= \Gamma\left(\underbrace{\left(\frac{I_2(t)}{2}\right)^2}_{\text{mutant} \times \text{mutant}} + \frac{1}{2} \times \underbrace{2 \times \frac{I_1(t)}{2}\frac{I_2(t)}{2}}_{\text{resident} \times \text{mutant}} \right). \end{aligned} \tag{11}$$

Taking into account interseason survival and primary infections results in the following discrete part:

$$\begin{cases} I_1[(n+1)T] = \chi_1 [I_1(nT+\tau)^2 + I_1(nT+\tau) I_2(nT+\tau)], \\ I_2[(n+1)T] = \chi_2 [I_2(nT+\tau)^2 + I_1(nT+\tau) I_2(nT+\tau)], \end{cases} \tag{12}$$

where $\chi_i = (\theta/\xi)(\Gamma/4) e^{-\mu_i (T-\tau)}$ and $\mu_i = f(\beta_i)$, for $i = 1, 2$.

When no mutant is present, the dynamics of a resident population with trait β_1 are governed by equations ([6]–[7]) and therefore converge to a T-periodic invariant solution, $I_1^\circ(t, \beta_1)$ ("Strong Allee Effect"). Since the mutant is rare initially ($I_2 \ll I_1$), its effects on the resident dynamics are negligible at first. During the first season

$$\dot{I}_2 \approx \beta_2 I_2 (N - I_1^\circ),$$

$$I_2(T) \approx \chi_2 I_1^\circ(\tau, \beta_1) I_2(\tau).$$

Let $\bar{I}_1^\circ = (1/\tau) \int_0^\tau I_1^\circ(t, \beta_1) \mathrm{d}t$, so that $N - \bar{I}_1^\circ$ denotes the mean susceptible host density at mutant-free equilibrium. We thus have $I_2(\tau) \approx I_2(0) e^{\beta_2 \tau (N - \bar{I}_1^\circ)}$. The mutant can invade provided that $I_2(T) > I_2(0)$, which reads

$$\frac{I_2(T)}{I_2(0)} \approx I_1^\circ(\tau, \beta_1) \times \chi_2 e^{\beta_2 \tau (N - \bar{I}_1^\circ)} > 1, \tag{13}$$

whereas if this quantity is less than 1, the mutant becomes extinct.

It is worth noting that the above invasion criterion is determined by two variables shaped by the resident trait, that is, mean susceptible host density $(N - \bar{I}_1^\circ)$ and infected host density at the end of the season $I_1^\circ(\tau, \beta_1)$. Moreover, there is a positive relationship between the end-of-season resident population density and the mutant reproductive success. Because the mutant is initially rare, it mainly mates with the resident. As a consequence, higher end-of-season resident population density results in more frequent mutant sexual reproduction which enables it to overwinter.

Evolutionary Outcomes

By definition of the endemic equilibrium, one has

$$\frac{I_1^\circ(T)}{I_1^\circ(0)} = I_1^\circ(\tau, \beta_1) \times \chi_1 e^{\beta_1 \tau (N - \bar{I}_1^\circ)} = 1. \tag{14}$$

Therefore, the invasion criterion (13) reads

$$\frac{I_2(T)}{I_2(0)} \approx \frac{\chi_2 e^{\beta_2 \tau (N - \bar{I}_1^\circ)}}{\chi_1 e^{\beta_1 \tau (N - \bar{I}_1^\circ)}} > 1. \tag{15}$$

We can thus derive an invasion fitness function as

$$\begin{aligned} s(\beta_1, \beta_2) &= (\beta_2 - \beta_1)(N - \bar{I}_1^\circ(\beta_1))\tau \\ &\quad - (f(\beta_2) - f(\beta_1))(T - \tau). \end{aligned} \tag{16}$$

The invasion fitness $s(\beta_1, \beta_2)$ is positive if phenotype β_2

can invade resident phenotype β_1; it is negative otherwise. The (β_1, β_2) pairs for which the mutant initially invades or not are illustrated in pairwise invasibility plots (PIP; figs. 3*A*, 4*A*, 5*A*, and 6*A*).

Under the trade-off hypothesis, there may exist ranges of β trait values where ecological dynamics of a monomorphic population converge to the disease-free equilibrium which is the only stable equilibrium (illustrated with light gray zones in figs. 3*B*, 4*B*, 5*B*, and 6*B*). These phenotypic ranges are henceforth referred to as a monomorphic extinction zones.

A necessary condition for a monomorphic population to split into a dimorphic population is given by

$$\left.\frac{\partial^2}{\partial \beta_2^2} s(\beta_1, \beta_2)\right|_{\beta_1=\beta_2=\beta} = -f''(\beta)(T-\tau) > 0. \quad (17)$$

Hence, evolutionary branching is conditioned by the concavity of the trade-off function: it can only occur under concave trade-off shapes ($f'' < 0$).

Numerical simulations performed for model ([10]–[12]), using the algorithm detailed in appendix B.2 and implemented in MATLAB, version R2012b (supplementary material, available online), showed that under convex trade-offs, any initial population with β value above the monomorphic extinction zone continuously evolves to-

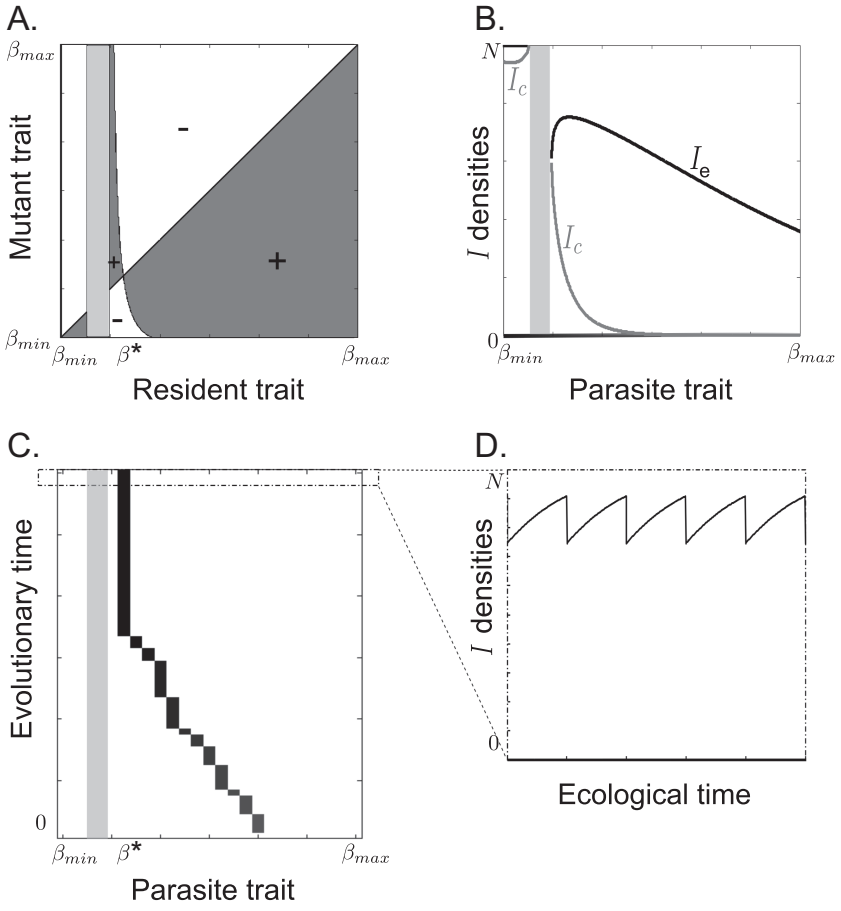

Figure 3: Evolutionary process leading to a monomorphic evolutionary endpoint ("Evolutionary Outcomes"). *A*, Pairwise invasibility plot. Areas where the mutant can invade are in dark gray. *B*, Equilibria in the mutant-free ecological model, as a function of the resident trait: disease-free equilibrium ($I = 0$, stable), I_c (unstable) and I_e (stable) or saturation ($I = N$, stable); black and gray colors correspond to stable and unstable equilibria, respectively. *C*, Associated evolutionary dynamics; numerical simulations were realized using an algorithm that is described in appendix B.2. The light gray areas (in *A*–*C*) correspond to resident trait values for which the endemic equilibrium I_e does not exist, that is, to a monomorphic extinction zone (apps. A.2, B; *B*). *D*, Ecological dynamics at evolutionary endpoint. For all panels, we used the following trade-off form: $\mu = f(\beta) = c\beta^a$, here $a = 1.2$ (trade-off shape: convex) and $c = 0.25$ (trade-off coefficient), $\beta_{min} = 0$ and $\beta_{max} = 6$ (phenotypic boundaries), $T = 1.5$ (time unit), $\tau = 1$ (time unit), $N = 1$ (host unit), $\theta = 1.06$ (per primary inoculum unit per unit time), $\xi = 1$ (per host unit per unit time), $\Gamma = 4$ (per squared host unit per unit time).

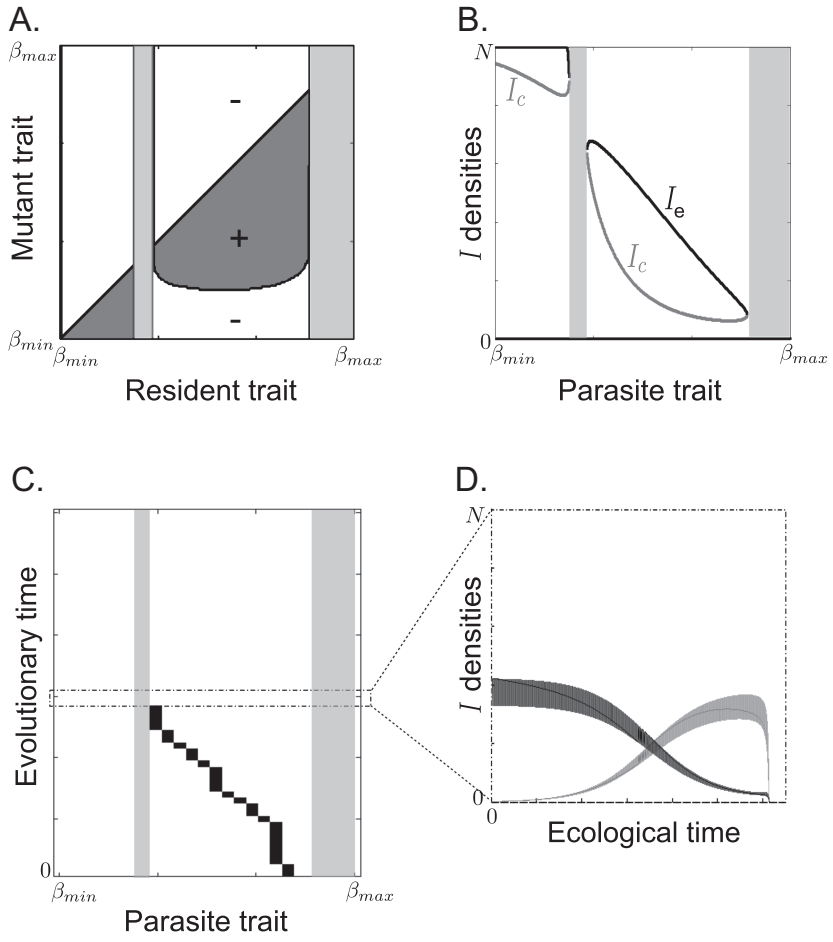

Figure 4: Evolutionary process leading to extinction. We refer the reader to figure 3's caption since the only change concerns the trade-off shape parameter: here, $a = 2.5$ (more convex trade-off). Also, we took $\beta_{max} = 3$ for illustrative purposes. Last, *D* shows ecological dynamics right before the evolutionary endpoint (extinction), that is, from the last mutation preceding extinction and over a far greater number of seasons than in figure 3*D*.

ward a singular trait value $\beta^\star$.[1] Provided reaching $\beta^\star$ does not require entering an extinction zone, the population monomorphically converges and stabilizes to $\beta^\star$ trait value (figure 3*C*, 3*D*). By contrast, whenever reaching $\beta^\star$ requires entering into a monomorphic extinction zone, the population becomes extinct (fig. 4*C*, 4*D*). The density of the mutant increases at first, taking advantage of the presence of the resident. During this phase, the resident population decreases to extinction. The mutant eventually predominates but it also becomes extinct as it is unable to survive alone.

A concave trade-off is a necessary yet not sufficient condition for an initially monomorphic population to evolve toward a branching point. When it does, as predicted by the PIP from figure 5*A*, the parasite population splits into a morph investing decreasingly into asexual reproduction (morph [a]), and a morph doing the opposite (morph [b]). This dimorphism allows morph (a) to cross the monomorphic extinction zone, because morph (b) provides it with mating opportunities. Morph (a) then becomes exclusively sexual ($\beta_{min} = 0$). The higher density corresponds to the ecological dynamics of an exclusively sexual morph (a), with a cyclic parthenogen (b) occuring at lower densities. For large β_{max} values, the cyclic parthenogen can also become extinct, and the population becomes exclusively sexual (fig. 6*B*). The relative increase in morph (b) density benefits the exclusively sexual morph (a), which ends up saturating the environment and excluding morph (b). Such unilateral extinction is made possible by the fact that morph (a) reached the critical pop-

1 Code that appears in the *American Naturalist* is provided as a convenience to the readers. It has not necessarily been tested as part of the peer review.

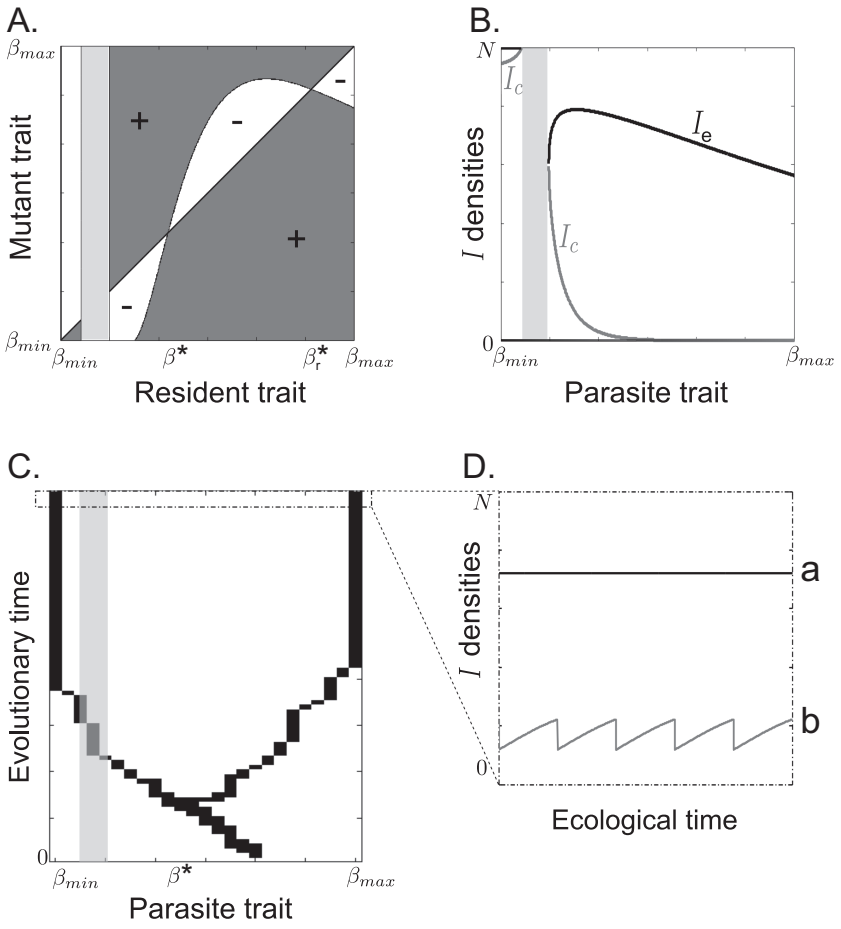

Figure 5: Evolutionary branching process leading to a dimorphic evolutionary endpoint ("Evolutionary Outcomes"). We refer the reader to figure 3's caption since the only change concerns the trade-off shape parameter: here, $a = 0.9$ (concave trade-off).

ulation density to be able to survive alone ($I_e > I_c$ for $\beta = 0$; see figs. 6*B* and 7).

Discussion

Strong Allee Effect and Evolutionary Extinction

That the component Allee effect linked to obligate mating causes a strong demographic Allee effect in cyclic parthenogens is an important conclusion of this work. This may lead the population to evolve to trait values where persistence is no longer possible, a phenomenon that has been termed "evolutionary extinction" or "evolutionary suicide" (Webb 2003; Parvinen 2005). Whether or not these critical parameter ranges can be reached in nature is not yet known. One may imagine that these ecological and evolutionary consequences of mate limitation might ultimately explain why many species in temperate areas do not undergo obligate sexual reproduction at the end of the season but rather adopt a mixed sexual-asexual survival strategy (Barrett et al. 2008).

A Novel Mechanism Promoting Variability in Reproductive Strategies

Allee effects, that is, positive density dependence, can promote evolutionary diversification as well. Indeed, we showed that obligate sexual reproduction makes the invasion fitness depend on both the mean resident density and the resident end-of-season density, which act on mutant invasion fitness in opposite ways. The mean resident density decreases mutant fitness, since both compete for susceptible hosts; the end-of-season resident density increases mutant fitness because it enables the mutant to generate survival forms through sexual reproduction.

Under convex transmission-survival trade-offs, these opposite effects select for a mixed sexual-asexual reproduction in cyclic parthenogens. The corresponding inter-

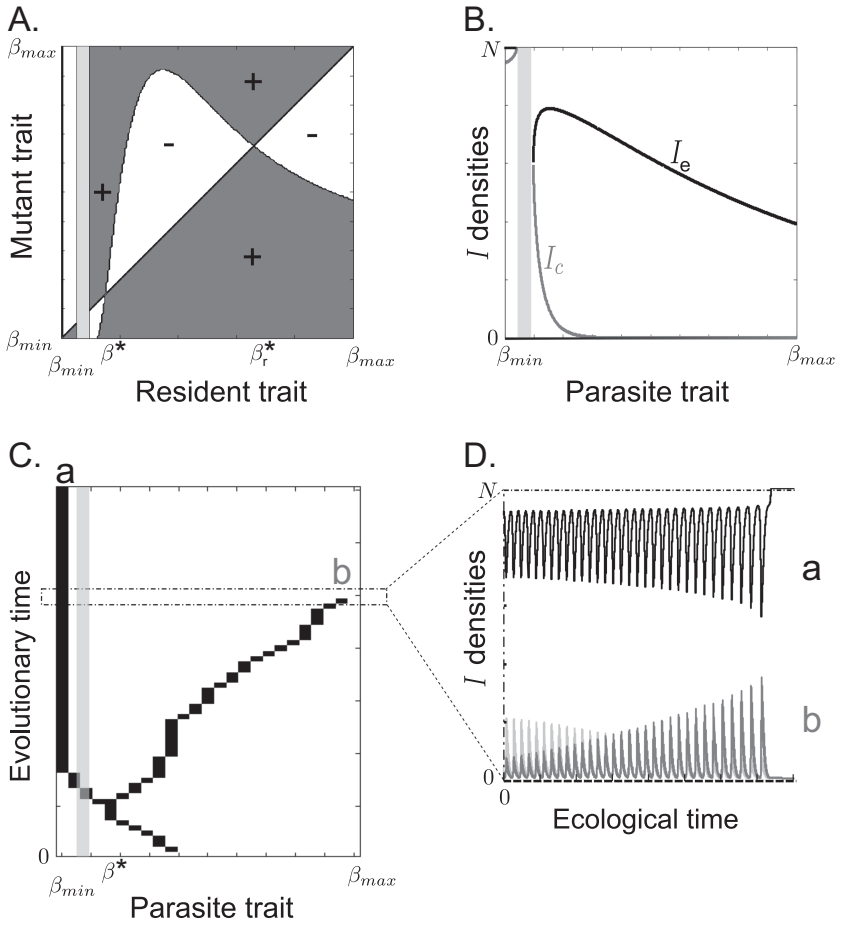

Figure 6: Evolutionary process leading to extinction of one branch. We refer the reader to figure 3's caption since the only changes concern the trade-off parameters: here, $a = 0.9$ (concave trade-off) and $c = 0.21$ (this deviation from fig. 5 is for illustrative purposes only). However, we took $\beta_{max} = 10$ (compared to 6 in fig. 5) to get extinction. Last, *D* shows ecological dynamics right before the evolutionary endpoint (extinction of one branch) over a far greater number of seasons than in figure 3*D*.

mediate investment into asexual reproduction has to be large enough to overcome Allee effects but small enough to ensure sexual survival. By contrast, under concave trade-offs, selection is disruptive and the population may undergo evolutionary branching.

After evolutionary branching occurs, continual phenotypic divergence is observed. Thus, the population comprises a cyclical parthenogenetic morph with both high asexual reproduction rate and low survival ability and an exclusively sexual morph, with high survival. When maintained, such a dimorphism is a "tragedy of the commune" (Doebeli et al. 2004). Evolution leads to an asymmetric state in which asexual morphs make cooperative investments in population density (a common good given the strong Allee effect) at the expense of a lower survival, while sexual morphs invest nothing, survive better, and eventually reach higher densities.

Transitions from Cyclical Parthenogenesis to Strict Sexual Reproduction

Evolution may alternatively drive the asexual morph to extinction. Although the sexual morph has maximal survival capacities, it cannot survive as a single morph before it has reached a quite elevated critical Allee density. During the transition, the sexual morph benefits from the presence of the asexual morph as it increases sexual reproduction opportunities. Once the sexual morph has grown above the Allee threshold, it may eventually exclude the asexual morph. Such a phenomenon is termed "evolutionary murder" by some authors (Parvinen 2005). Asexual reproduction can thus be an evolutionary transient state leading to strict sexual reproduction. A similar phenomenon is highlighted by Boldin and Kisdi (2012), who show that evolutionary branching can ultimately select for a single

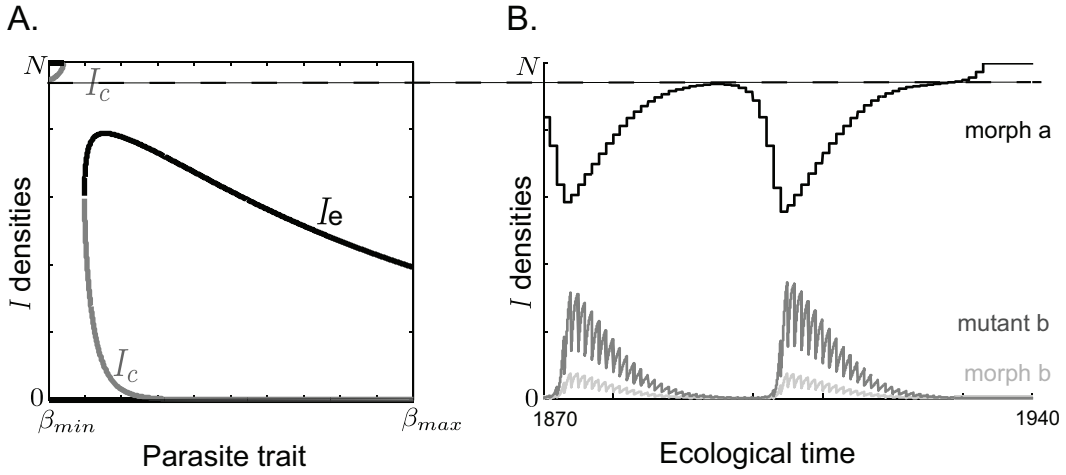

Figure 7: Zoom on exclusion dynamics in figure 6. *A*, Ecological equilibria for a mutant-free monomorphic population as a function of the parasite trait β: the disease-free equilibrium $I = 0$ and the endemic equilibria $I = I_e$ and $I = N$ (saturation) are stable (black lines), while $I = I_c$ is unstable (gray line). The light gray area corresponds to a monomorphic extinction zone (apps. A.2, B). *B*, Ecological dynamics leading to morph (b) exclusion. The black and gray lines correspond to morph (a) and (b) dynamics, respectively. The darker gray line corresponds to the mutant arising from morph (b). We refer the reader to figure 6's caption for parameter values.

parasite strain which excels in transmission via free-living forms. An open-ended question is whether such complex evolutionary transitions might happen in nature. Phylogenetic reconstructions of character states may help with this issue, provided that adaptation is a slow process, long-lasting enough to be detected by phylogenetic methods.

Disentangling Ultimate Causes of Reproductive Polymorphism

Possible mechanisms for polymorphism in sexual mode of reproduction include (i) temporal variation in winter survival rates (Simon et al. 2002), (ii) local adaptation to fine-scale spatial variation (Kawecki and Ebert 2004), and (iii) Allee effects associated with obligate sexual reproduction, as shown in this study.

From their analysis of *Leptosphaeria maculans* populations, Dilmaghani et al. (2012) suggest that polymorphism in sexual mode of reproduction may be related to climatic conditions in Saskatchewan province, which is akin to (i). In *Melampsora larici-populina*, Xhaard et al. (2011) suggest that sexual and almost asexual lineages evolved at the ends of an altitudinal gradient and happen to co-occur at intermediate positions in the gradient, which is akin to (ii). Alternatively, it may be that in both species, polymorphism results from (iii), Allee effects and obligate sexual reproduction.

Distinguishing between adaptive hypotheses can be challenging. Testing adaptation to temporal variability in winter survival rates requires relating the variance in reproductive strategies to climatic data as exemplified by Halkett et al. (2004) in aphids. Testing whether polymorphism in reproductive strategies is selected as a local adaptation in a spatially heterogeneous environment implies reciprocal transplantations (Lenormand 2002). If this mechanism is not involved, sexual and almost asexual lineages should perform as well in every tested environment. Testing whether Allee effects explain variability could be done by experimentally manipulating morph frequencies, such as testing an advantage of the rarest in dimorphic plants (Gigord et al. 2001).

Lastly, an alternative mechanism for polymorphism involves multiple infections, as shown by by Alizon and van Baalen (2008) and Boldin and Diekmann (2008). Given a reasonably sensitive genetic marker, it might be feasible to test this hypothesis (López-Villavicencio et al. 2011).

Perspectives

From a broader perspective, our study may shed light on the coexistence of male- and non-male-producing clones in cyclic parthenogens such as *Daphnia* (Galimov et al. 2011). Producing males is likely a costly venture. However, non-male-producing morphs still have to mate with male-producing morphs to complete their life cycle. In our study, strictly sexual morphs similarly depend on cyclic parthenogens for obligate mating to take place. By the same token, non-male-producing morphs (defectors) may indeed coexist with male-producing morphs (cooperators).

Since we considered sexual reproduction obligate, our

model has not been designed to analyze whether sexual reproduction can outcompete asexual reproduction on an evolutionary timescale. Nevertheless, the mechanism involved in the loss of a dual reproductive mode toward exclusive sexual reproduction highlights the fact that complex dynamics may lead cyclic parthenogens to become exclusively sexual. Further studies may reconsider the hypothesis of an exclusively sexual overwintering survival and investigate asexual survival possible as well. This would pave the way toward addressing the emergence and the coexistence of exclusively sexual and exclusively asexual lineages in nature, as well as the possible loss of sex.

Acknowledgments

M.C. is supported by a PhD fellowship from the Institut National de la Recherche Agronomique "Plant Health and the Environment" Division and the Council of Brittany region. We thank F. Halkett for insightful discussions about the biology of fungal plant pathogens. We are also grateful to two anonymous reviewers for their useful comments. For this work, V.R. benefited from funds from project BIOFIS (reference 1001-001) of the Agropolis Fondation (Montpellier, France). This work was supported by a grant overseen by the French National Research Agency (ANR) as part of the "Blanc 2013" program (ANR-13-BSV7-0011, FunFit project). Thanks to I. Mascio for her help in the English editing.

APPENDIX A
Ecological Model

A.1. Derivation of Equation (5)

Here we briefly present the aggregation technique proposed by Mailleret et al. (2012) to reduce semidiscrete seasonal epidemic models. This technique is based on the hypothesis that primary infections occur on a faster timescale than secondary infections. A full in-season model accounting for primary infections, primary inoculum depletion, and secondary infections reads

$$\begin{aligned}
\dot{P} &= -\frac{\xi}{\varepsilon} SP,\\
\dot{S} &= -\frac{\theta}{\varepsilon} SP - \beta S(I_- + I_+),\\
\dot{I}_- &= \frac{1}{2}\frac{\theta}{\varepsilon} SP + \beta S I_-,\\
\dot{I}_+ &= \frac{1}{2}\frac{\theta}{\varepsilon} SP + \beta S I_+,
\end{aligned}$$

where each primary infection generates "−" or "+" infected hosts in equal probability. Parameters ξ and θ are associated with primary inoculum depletion and primary infections, and ε is a scaling factor. At the beginning of the season $S[(n+1)T] = N$, $I_+[(n+1)T] = 0$, $I_-[(n+1)T] = 0$ and $P[(n+1)T] > 0$.

Assuming that primary infections occur on a faster time-scale than secondary infections amounts to considering that ε is small. Rewriting the model in the timescale corresponding to primary infections ($t' = t/\varepsilon$), and neglecting the terms inε, the model reads:

$$\begin{aligned}
P' &= -\xi SP,\\
S' &= -\theta SP,\\
I' &= \theta SP,
\end{aligned}$$

with the prime indicating derivatives with respect to t' and $I = I_+ + I_-$. Thus, on the timescale of primary infections, the quantity $S - (\theta/\xi)P$ remains equal to $N - (\theta/\xi) \times P[(n+1)T]$, so that one has

$$S' = -\xi S\left(S - \left\{N - \frac{\theta}{\xi} P[(n+1)T]\right\}\right).$$

Since $S[(n+1)T] = N > 0$, S converges to $\max(0, N - (\theta/\xi)P((\mathrm{n}+1)T))$ over the timescale of primary infections. Accordingly, since $S + I = N$, I converges to $\min\{(\theta/\xi)P[(n+1)T],\mathrm{N}\}$ over the timescale of primary infections. When the primary inoculum is very infectious (large θ/ξ), it can infect every susceptible hosts during the primary infection phase. When θ/ξ is small, primary infections result in the linear conversion of primary inoculum into infected host, as in equation (5), resulting in model (8).

A.2. Equilibria

Model (8)'s equilibria are fixed points $I^* = m(I^*)$ of the discrete-time map m: $I_n \mapsto I_{n+1}$ from equation (8). The disease-free equilibrium (DFE) $I = 0$ is a trivial fixed point. Apart from the DFE, other equilibria may exist, depending on the following conditions.

If $\beta = 0$, one finds one additional fixed point: $I = 1/\chi$. Otherwise ($\beta > 0$), two additional fixed points may exist, provided that

$$\Delta = \chi N[\chi N - 4\mathrm{e}^{-\beta N\tau}(1 - \mathrm{e}^{-\beta N\tau})] > 0. \tag{A1}$$

Let

$$\begin{aligned}
I_c &= \frac{N}{2}\frac{\chi N - 2\mathrm{e}^{-\beta N\tau}(1 - \mathrm{e}^{-\beta N\tau}) - \sqrt{\Delta}}{(\mathrm{e}^{-\beta N\tau} - 1)^2},\\
I_e &= \frac{N}{2}\frac{\chi N - 2\mathrm{e}^{-\beta N\tau}(1 - \mathrm{e}^{-\beta N\tau}) + \sqrt{\Delta}}{(\mathrm{e}^{-\beta N\tau} - 1)^2},
\end{aligned} \tag{A2}$$

thereafter referred to as critical and endemic equilibrium densities, respectively. One can easily check that $\Delta > 0$ implies that $I_e > I_c > 0$.

An equilibrium I^* is stable if $|m'(I^*)| < 1$ and unstable if $|m'(I^*)| > 1$. Since $m'(0) = 0$, the DFE $[f(0) = 0]$ is stable in any event. Similarly, one can notice that for $\beta = 0$, $m'(1/\chi) = 2$ so that this nongeneric fixed point is always unstable. Moreover, one can easily check that m is a continuous and strictly increasing function, so that a graphical analysis suffices to show that I_c and I_e are unstable and stable, respectively (fig. 2).

APPENDIX B

Phenotypic Competition and Evolution

B.1. Competition Model

Considering a set of phenotypes $\{\beta_i\}$, $i = 1, 2, ..., n$, the in-season competition model reads

$$\dot{P}_i = -\frac{\xi}{\varepsilon} SP_i,$$

$$\dot{S} = -\sum_j \frac{\theta}{\varepsilon} SP_j - \sum_j \beta_j SI_j,$$

$$\dot{I}_i = \frac{\theta}{\varepsilon} SP_i + \beta_i SI_i.$$

Proceeding as in appendix A.1 and noticing that $r_i = P_i / \sum_j P_j$ is a constant, we obtain, during the season,

$$\dot{S} = -\sum_j \beta_j SI_j,$$

$$\dot{I}_i = +\beta_i SI_i, \tag{B1}$$

and from season to season:

$$S[(n+1)T] = \max\left\{N - \frac{\theta}{\xi}\sum_j P_j[(n+1)T], 0\right\},$$

$$I_i[(n+1)T] = \min\left\{\frac{\theta}{\xi} P_i[(n+1)T], N \times \frac{P_i[(n+1)T]}{\sum_j P_j[(n+1)T]}\right\}, \tag{B2}$$

where

$$P_i[(n+1)T] = \frac{\Gamma}{4} e^{-\mu_i(T-\tau)}[I_i(nT+\tau)\sum_j I_j(nT+\tau)]; \tag{B3}$$

see equation (11). When θ/ξ is small, primary infections result in the linear conversion of primary inoculum into infected hosts, with I_i tending to $(\theta/\xi)P_i[(n+1)T]$, which leads to equation (12). Evolutionary computations were actually realized using the full model, equations (B1)–(B3).

B.2. Evolution Algorithm

The evolving phenotype β ranges from 0 to β_{max}. This interval is divided into a finite number of subintervals ($n = 25$). Simulations start from a monomorphic population having a given β trait value. Once at ecological attractor, which we compute as the solution of the full competition model after a fixed horizon of 10,000 years, a small mutation occurs, having an equal probability of being on the left (smaller β) or on the right (larger β), regardless the subinterval considered. Then the process reiterates.

Literature Cited

Abang, M. M., M. Baum, S. Ceccarelli, S. Grando, C. C. Linde, A. Yahyaoui, J. Zhan, and B. A. McDonald. 2006. Differential selection on *Rhynchosporium secalis* during parasitic and saprophytic phases in the barley scald disease cycle. Phytopathology 96:1214–1222.

Abrahamson, W. G. 1980. Demography and vegetative reproduction. Pages 89–106 *in* O. Solbrig, ed. Demography and evolution in plant populations. University of California Press, Berkeley.

Alizon, S., and M. van Baalen. 2008. Multiple infections, immune dynamics, and the evolution of virulence. American Naturalist 172: E150–E168.

Allee, W. C., A. E. Emerson, O. Park, T. Park, and K. P. Schmidt. 1949. Principles of animal ecology. Saunders, Philadelphia.

Anderson, R. M., and R. M. May. 1991. Infectious diseases of humans: dynamics and control. Oxford University Press, Oxford.

Bailey, D. J., and C. A. Gilligan. 1999. Dynamics of primary and secondary infection in take-all epidemics. Phytopathology 89:84–91.

Barrett, L. G., P. H. Thrall, J. J. Burdon, A. B. Nicotra, and C. C. Linde. 2008. Population structure and diversity in sexual and asexual populations of the pathogenic fungus *Melampsora lini*. Molecular Ecology 17:3401–3415.

Billiard, S., M. López-Villavicencio, B. Devier, M. E. Hood, C. Fairhead, and T. Giraud. 2011. Having sex, yes, but with whom? inferences from fungi on the evolution of anisogamy and mating types. Biological Reviews 86:421–442.

Boldin, B., and O. Diekmann. 2008. Superinfections can induce evolutionarily stable coexistence of pathogens. Journal of Mathematical Biology 56:635–672.

Boldin, B., and E. Kisdi. 2012. On the evolutionary dynamics of pathogens with direct and environmental transmission. Evolution 66:2514–2527.

Caraco, T., and I. Wang. 2008. Free-living pathogens: life-history constraints and strain competition. Journal of Theoretical Biology 250:569–579.

Carmona, M. J., N. Dimas-Flores, E. M. García-Roger, and M. Serra. 2009. Selection of low investment in sex in a cyclically parthenogenetic rotifer. Journal of Evolutionary Biology 22:1975–1983.

Carson, M. L. 1998. Aggressiveness and perennation of isolates of *Cochliobolus heterostrophus* from north carolina. Plant Disease 82: 1043–1047.

Chamberlain, M., S. Ertz, and D. S. Ingram. 1995. Effect of extracts

of *Pyrenopeziza brassicae* on the reproductive development of other species of fungi. Mycologia 87:846–856.

Chamberlain, M., and D. Ingram. 1997. The balance and interplay between asexual and sexual reproduction in fungi. Pages 71–87 *in* J. H. Andrews, I. C. Tommerup, and J. A. Callow, eds. Advances in Botanical Research. Vol. 24. Academic Press, San Diego, CA.

Coluccio, A. E., R. K. Rodriguez, M. J. Kernan, and A. M. Neiman. 2008. The yeast spore wall enables spores to survive passage through the digestive tract of *Drosophila*. PLoS ONE 3:e2873.

Davis, H. G., C. M. Taylor, J. G. Lambrinos, and D. R. Strong. 2004. Pollen limitation causes an Allee effect in a wind-pollinated invasive grass (*Spartina alterniflora*). Proceedings of the National Academy of Sciences of the USA 101:13804–13807.

Day, T. 2002. Virulence evolution via host exploitation and toxin production in spore-producing pathogens. Ecology Letters 5:471–476.

Day, T., and K. A. Young. 2004. Competitive and facilitative evolutionary diversification. BioScience 54:101–109.

De Paepe, M., and F. Taddei. 2006. Viruses' life history: towards a mechanistic basis of a trade-off between survival and reproduction among phages. PLoS Biology 4:e193.

Dieckmann, U., and R. Law. 1996. The dynamical theory of coevolution: a derivation from stochastic ecological processes. Journal of Mathematical Biology 34:579–612.

Diekmann, O. 2004. A beginner's guide to adaptative dynamics. Banach Center 63:47–86.

Dilmaghani, A., P. Gladieux, L. Gout, T. Giraud, P. C. Brunner, A. Stachowiak, M. Balesdent, and T. Rouxel. 2012. Migration patterns and changes in population biology associated with the worldwide spread of the oilseed rape pathogen *Leptosphaeria maculans*. Molecular Ecology 21: 2519–2533.

Doebeli, M. 2011. Adaptive diversification. Princeton University Press, Princeton, NJ.

Doebeli, M., and U. Dieckmann. 2000. Evolutionary branching and sympatric speciation caused by different types of ecological interactions. American Naturalist 156(suppl.):S77–S101.

Doebeli, M., C. Hauert, and T. Killingback. 2004. The evolutionary origin of cooperators and defectors. Science 306:859–862.

Elam, D. R., C. E. Ridley, K. Goodell, and N. C. Ellstrand. 2007. Population size and relatedness affect fitness of a self-incompatible invasive plant. Proceedings of the National Academy of Sciences of the USA 104:549–552.

Fabre, F., E. Rousseau, L. Mailleret, and B. Moury. 2012. Durable strategies to deploy plant resistance in agricultural landscapes. New Phytologist 193:1064–1075.

Galimov, Y., B. Walser, and C. R. Haag. 2011. Frequency and inheritance of non-male producing clones in *Daphnia magna*: evolution towards sex specialization in a cyclical parthenogen? Journal of Evolutionary Biology 24:1572–1583.

Gandon, S. 1998. The curse of the pharaoh hypothesis. Proceedings of the Royal Society B: Biological Sciences 265:1545–1552.

Garrett, K. A., and R. L. Bowden. 2002. An Allee effect reduces the invasive potential of *Tilletia indica*. Phytopathology 92:1152–1159.

Gascoigne, J., L. Berec, S. Gregory, and F. Courchamp. 2009. Dangerously few liaisons: a review of mate-finding Allee effects. Population Ecology 51:355–372.

Gigord, L. D. B., M. R. Macnair, and A. Smithson. 2001. Negative frequency-dependent selection maintains a dramatic flower color polymorphism in the rewardless orchid *Dactylorhiza sambucina* (L.) Soò. Proceedings of the National Academy of Sciences of the USA 98:6253–6255.

Halkett, F., R. Harrington, M. Hullé, P. Kindlmann, F. Menu, C. Rispe, and M. Plantegenest. 2004. Dynamics of production of sexual forms in aphids: theoretical and experimental evidence for adaptive "coin flipping" plasticity. American Naturalist 163:E112–E125.

Hamelin, F., M. Castel, S. Poggi, D. Andrivon, and L. Mailleret. 2011. Seasonality and the evolutionary divergence of plant parasites. Ecology 92:2159–2166.

Heitman, J., J. W. Kronstad, J. W. Taylor, and L. A. Casselton. 2007. Sex in fungi: molecular determination and evolutionary implications. American Society for Microbiology, Washington, DC.

Kawecki, T. J., and D. Ebert. 2004. Conceptual issues in local adaptation. Ecology Letters 7:1225–1241.

Kramer, A. M., B. Dennis, A. M. Liebhold, and J. M. Drake. 2009. The evidence for Allee effects. Population Ecology 51:341–354.

Krkošek, M., B. M. Connors, M. A. Lewis, and R. Poulin. 2012. Allee effects may slow the spread of parasites in a coastal marine ecosystem. American Naturalist 179:401–412.

Lenormand, T. 2002. Gene flow and the limits to natural selection. Trends in Ecology and Evolution 17:183–189.

López-Villavicencio, M., F. Courjol, A. K. Gibson, M. E. Hood, O. Jonot, J. A. Shykoff, and T. Giraud. 2011. Competition, cooperation among kin, and virulence in multiple infections. Evolution 65:1357–1366.

Mailleret, L., M. Castel, J. Montarry, and F. M. Hamelin. 2012. From elaborate to compact seasonal plant epidemic models and back: is competitive exclusion in the details? Theoretical Ecology 5:311–324.

Mailleret, L., and V. Lemesle. 2009. A note on semi-discrete modelling in the life sciences. Philosophical Transactions of the Royal Society A: Mathematical, Physical and Engineering Sciences 367:4779–4799.

Metz, J., R. Nisbet, and S. Geritz. 1992. How should we define "fitness" for general ecological scenarios? Trends in Ecology and Evolution 7:198–202.

Michelmore, R., and D. Ingram. 1980. Heterothallism in *Bremia lactucae*. Transactions of the British Mycological Society 75:47–56.

Parvinen, K. 2005. Evolutionary suicide. Acta Biotheoretica 53:241–264.

Schoustra, S., H. D. Rundle, R. Dali, and R. Kassen. 2010. Fitness-associated sexual reproduction in a filamentous fungus. Current Biology 20:1350–1355.

Simon, J., C. Rispe, and P. Sunnucks. 2002. Ecology and evolution of sex in aphids. Trends in Ecology and Evolution 17:34–39.

Sommerhalder, R. J., B. A. McDonald, F. Mascher, and J. Zhan. 2010. Sexual recombinants make a significant contribution to epidemics caused by the wheat pathogen *Phaeosphaeria nodorum*. Phytopathology 100:855–862.

———. 2011. Effect of hosts on competition among clones and evidence of differential selection between pathogenic and saprophytic phases in experimental populations of the wheat pathogen *Phaeosphaeria nodorum*. BMC Evolutionary Biology 11:188.

Tessier, A. J., and C. E. Cáceres. 2004. Differentiation in sex investment by clones and populations of *Daphnia*. Ecology Letters 7: 695–703.

Vallejo-Marín, M., M. E. Dorken, and S. C. Barrett. 2010. The ecological and evolutionary consequences of clonality for plant mat-

ing. Annual Review of Ecology, Evolution, and Systematics 41: 193–213.

van den Berg, F., N. Bacaer, J. Metz, C. Lannou, and F. van den Bosch. 2011. Periodic host absence can select for higher or lower parasite transmission rates. Evolutionary Ecology 25:121–137.

Vercken, E., A. M. Kramer, P. C. Tobin, and J. M. Drake. 2011. Critical patch size generated by Allee effect in gypsy moth, *Lymantria dispar* (L.). Ecology Letters 14:179–186.

Webb, C. 2003. A complete classification of Darwinian extinction in ecological interactions. American Naturalist 161:181–205.

Williams, G. C. 1975. Sex and evolution. Princeton University Press, Princeton, NJ.

Wittmann, M. J., M. A. Lewis, J. D. Young, and N. D. Yan. 2011. Temperature-dependent Allee effects in a stage-structured model for *Bythotrephes* establishment. Biological Invasions 13:2477–2497.

Xhaard, C., B. Fabre, A. Andrieux, P. Gladieux, B. Barrès, P. Frey, and F. Halkett. 2011. The genetic structure of the plant pathogenic fungus *Melampsora larici-populina* on its wild host is extensively impacted by host domestication. Molecular Ecology 20: 2739–2755.

Associate Editor: Benjamin Bolker
Editor: Troy Day